

---

# SemFlow: Binding Semantic Segmentation and Image Synthesis via Rectified Flow

---

Chaoyang Wang<sup>1</sup>, Xiangtai Li<sup>2</sup>, Lu Qi<sup>3</sup>, Henghui Ding<sup>2</sup>  
Yunhai Tong<sup>1</sup>, Ming-Hsuan Yang<sup>3</sup>

<sup>1</sup>Peking University, <sup>2</sup>Nanyang Technological University, <sup>3</sup>UC, Merced

## Abstract

Semantic segmentation and semantic image synthesis are two representative tasks in visual perception and generation. While existing methods consider them as two distinct tasks, we propose a unified diffusion-based framework (SemFlow) and model them as a pair of reverse problems. Specifically, motivated by rectified flow theory, we train an ordinary differential equation (ODE) model to transport between the distributions of real images and semantic masks. As the training object is symmetric, samples belonging to the two distributions, images and semantic masks, can be effortlessly transferred reversibly. For semantic segmentation, our approach solves the contradiction between the randomness of diffusion outputs and the uniqueness of segmentation results. For image synthesis, we propose a finite perturbation approach to enhance the diversity of generated results without changing the semantic categories. Experiments show that our SemFlow achieves competitive results on semantic segmentation and semantic image synthesis tasks. We hope this simple framework will motivate people to rethink the unification of low-level and high-level vision. Project page: <https://github.com/wang-chaoyang/SemFlow>.

## 1 Introduction

Understanding semantic content and creating images from semantic conditions are fundamental research topics in computer vision. Semantic segmentation [48, 7, 62, 87, 11, 10] and image synthesis [8, 31, 26, 74, 91] are two representative dense prediction tasks and inspires various downstream applications, including autonomous driving [5] and medical image analysis [90]. The former aims to assign a category label to each pixel in the image, while the latter aims to generate realistic images given semantic layouts.

Although semantic segmentation and image synthesis constitute a pair of reverse problems, existing works typically solve them using two distinct methodologies. On the one hand, semantic segmentation models mostly follow the spirit of discriminative models. Specifically, a well-pre-trained backbone is employed to extract multi-scale features, and then a task-specific decoder is used for dense prediction. On the other hand, semantic image synthesis frameworks are mainly built upon generative adversarial networks (GAN) [17, 55, 60, 65] or diffusion models (DM) [66, 67, 23]. GAN-based methods [91, 74, 26] typically take semantic layouts as inputs and adopt a discriminator for adversarial training. Meanwhile, DM-based methods [39] generate from noise with a semantic layout functioning as a control signal.

An intuitive solution is to represent the segmentation mask as a colormap and model it as a conditional image generation task [59]. However, there are several implementation challenges. Overall, most of the discriminative segmentation models do not apply to this problem due to their irreversibility. For generative adversarial networks, their generators are typically unidirectional. Jointly training multiple unidirectional models to achieve bidirectional generation [91] is not the concern of this paper. Latent diffusion models (LDMs) have recently demonstrated great potential in generative tasks. Beyond

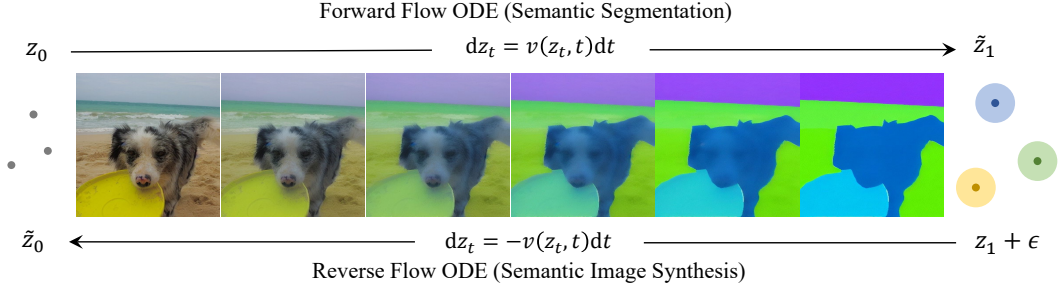


Figure 1: **Rectified flow bridges semantic segmentation (SS) and semantic image synthesis (SIS).** SS and SIS are modeled as a pair of transportation problems between the distributions of images and masks. They share the same ODE and only differ in the direction of the velocity field. We propose a finite perturbation operation on the mask to enable multi-modal generation without changing the semantic labels. *Grey dots* represent data samples. *Colored dots* represent semantic centroids, also known as anchors in Eq. 7. *Colored bubbles* represent the scale of perturbation.

generative tasks, several works [59, 71] attempt to apply diffusion models for segmentation, with images functioning as conditions, but their applicable tasks are limited to be class-agnostic. There are three main problems for existing LDM-based segmentation frameworks: 1) The contradiction between the randomness of generation outputs and the certainty of segmentation labels. 2) The huge cost brought by multiple inference steps. 3) The irreversibility between semantic masks and images.

In this paper, we use rectified flow [43, 45, 15] to enable LDM as a unified framework for semantic segmentation and semantic image synthesis. Our key idea is summarized in Fig. 1. Starting from an LDM [61] framework, we solve the above problems with three methodologies. First, we redefine the mapping function to address the randomness. Previous works [59] aim to learn the mapping from the joint distribution of Gaussian noise and images to the segmentation masks. We argue that Gaussian noise in this mapping function is redundant and negatively affects the determinism of semantic segmentation results. Instead, our model directly learns the mapping from images to masks. Secondly, we make the mapping reversible via rectified flow. Rectified flow is an ordinary differential equation (ODE) framework with a time-symmetric training object. This feature allows the model to be trained once to obtain bi-directional transmission capabilities and can be solved numerically using simple ODE solvers such as Euler. Finally, we propose a finite perturbation method to enable multi-modal image synthesis, as the mapping is one-to-one in semantic segmentation but one-to-many in semantic synthesis. We add amplitude-limited noise, enabling masks to be sampled from a collection of semantic-invariant distributions rather than a fixed value, and further improving the quality of synthesized results. Moreover, our model needs fewer inference steps than traditional diffusion models because the transport trajectory is straight, significantly reducing the gap between LDM and traditional discriminative models in segmentation.

The main contributions are as follows: 1) We introduce SemFlow, a new unified framework that binds semantic segmentation and image synthesis with rectified flow, effectively leveraging the length of the generative models. 2) We propose specialized designs of SemFlow, including pseudo mask modeling, bi-directional training of segmentation and generation, and a finite perturbation strategy. 3) We validate SemFlow on several popular benchmarks. For semantic segmentation, SemFlow greatly narrows the gap between diffusion models and discriminative models in terms of accuracy and inference speed with a more elegant framework. Meanwhile, SemFlow also performs decently in semantic image synthesis tasks.

## 2 Related Work

**Diffusion Models and Rectified Flow.** Diffusion models [23, 66, 67] have shown impressive results in the field of generation, such as image generation [61, 58, 85, 25, 13, 57], video generation [82], image editing [4, 49, 63, 54, 21], image super resolution [64, 24] and point cloud [50, 53, 89, 84, 51]. Most of these methods are based on stochastic differential equations (SDEs) and need multiple steps for generation. Recently, some works [43, 42, 41, 1, 20] propose to model with probability flow ordinary differential equations (ODEs) to reduce the inference steps. Specifically, rectified

flow [43, 45] defines the forward process as straight paths and uses reflow to minimize the sampling steps to one. Although rectified flow has demonstrated decent results on image generation and image transfer tasks, they are limited to low-level vision and lack an exploration of the unification of segmentation and generation tasks.

**Semantic Segmentation** is one of the core tasks in visual perception, aiming to assign each pixel of the given image a semantic category. Previous semantic segmentation approaches are typically built upon discriminative modeling, consisting of a strong backbone [19, 14, 46, 47] for feature extraction and a task-specific decoder head [7, 62, 87, 11, 10, 35, 32, 37, 36, 34] for mask prediction. Recently, some works [33, 88, 16, 79, 77, 3, 72, 9, 18, 2, 28, 78, 73] exploit diffusion models for segmentation. They typically follow the spirit of discriminative models and employ the diffusion model as a feature extractor. Although UniGS [59] and LDMSeg [71] attempt to use a plain Stable Diffusion framework for segmentation, their applicable tasks are limited to be class-agnostic. In practice, reconciling the stochastic outputs of diffusion models with the deterministic results of semantic segmentation is difficult. We rethink this problem and re-model it with rectified flow.

**Semantic Image Synthesis** is the reverse problem of semantic segmentation, aiming to generate realistic images given semantic layouts [8, 56, 44, 76, 92, 68, 69, 81, 31, 38, 52]. Several studies have delved into semantic synthesis through two methodologies. One methodology [91, 26, 74, 6, 70] is based on GAN and trained with adversarial loss and reconstruction loss. However, some of these methods can only generate unimodal outputs. Although some methods [69, 93] have been developed to address the diversity issues, GAN-based frameworks typically suffer from unstable training and need careful parameter tuning. Another methodology [75] employs diffusion models and regards it as a conditional image generation task, where semantic masks function as control signals. Some works further add a greater variety of control signals to enhance the consistency of synthesized results, like textual prompts [80] and bounding box [39]. Despite these methods achieving good synthetic results, their architecture is usually asymmetric, and the generator is usually unidirectional. This hinders the exploration of the unification of semantic segmentation and image synthesis.

### 3 Method

In this section, we first review diffusion models and the differential equations of diffusion-based segmentation models (DSMs) and then analyze the disadvantages of existing approaches. Afterward, we propose our SemFlow, which is inspired by rectified flow theory. It solves the randomness problem in the existing DSM and unifies semantic segmentation and image synthesis with *one* model. We will elaborate on each phase of our method.

#### 3.1 Diffusion Model and Segmentation Modeling.

Diffusion models are a class of likelihood-based models that define a Markov chain of forward and backward processes. In the forward process, the noise is gradually added to the real data  $x_0$  to form the noisy data  $x_t$ :

$$q(x_t|x_0) = \mathcal{N}(x_t; \sqrt{\alpha_t}x_0, (1 - \alpha_t)I), \quad (1)$$

where  $\alpha_t$  is functions of  $t$ . During training, the model  $\epsilon_\theta$  learns to estimate the noise by minimizing the objective with L2 loss:

$$\mathcal{L} = \mathbb{E}_{x_0 \sim q(x_0), \epsilon \sim \mathcal{N}(0, I), t} \left[ \left\| \epsilon_\theta(\sqrt{\alpha_t}x_0 + \sqrt{1 - \alpha_t}\epsilon_t, t) - \epsilon_t \right\|^2 \right], \quad (2)$$

In the backward process, the model starts from Gaussian noise and gradually denoises to generate realistic data [66] via,

$$x_{t-1} = \sqrt{\alpha_{t-1}} \left( \frac{x_t - \sqrt{1 - \alpha_t}\epsilon_\theta(x_t, t)}{\sqrt{\alpha_t}} \right) + \sqrt{1 - \alpha_{t-1} - \sigma_t^2}\epsilon_\theta(x_t, t) + \sigma_t\epsilon_t. \quad (3)$$

Luckily, Eq. 3 provides a unified solution for DDPM and DDIM, where the former belongs to an SDE modeling and the latter is an ODE modeling. We parameterized it as

$$x_0 = f(x_T, \sigma), \quad (4)$$

where  $\sigma$  controls the way of modeling:

$$\sigma_t = \begin{cases} \sqrt{(1 - \alpha_{t-1})(1 - \alpha_t)}\sqrt{1 - \alpha_t/\alpha_{t-1}} & \text{DDPM} \\ 0 & \text{DDIM} \end{cases} \quad (5)$$

In the image generation task,  $x_0$  represents the real images, and  $x_T$  represents the Gaussian noise. We extend the boundaries of Eq. 4 and apply it to semantic segmentation problems. An intuitive way is to encode the segmentation mask into colormaps and model segmentation as a conditional image generation task. Given image  $I$ , we rewrite the projection  $f$  into a formulation of conditional generation,

$$x_0 = f(x_T, \sigma, I). \quad (6)$$

Eq. 6 formulates the existing diffusion-based segmentation models with generative modeling. However, this modeling approach suffers from the following problems: 1) The randomness of initial noise and the determinism of the segmentation mask are contradictory. 2) From a transmission point of view, the transfer from noise to the segmentation mask does not conform to the paradigm of semantic segmentation task, where noise is redundant. 3) The images in this approach only serve as the condition, which is non-casual in reverse transfer. Thus, the reversed transfer is a separate problem.

### 3.2 Unify Segmentation and Synthesis with Rectified Flow

**Task-agnostic Framework.** We employ the standard Stable Diffusion [61] (SD) framework for our task without any task-specific decoder head or well-designed text prompts. To this end, we design the network architecture using the following three steps. First, we convert the semantic segmentation masks to 3-channel pseudo mask  $M = (m_0, m_1, m_2)$  to align with the images  $I$ . Assume that the valid region  $[0, 255]$  (for real images) is divided into  $k$  parts with a spacing of  $s$ , the pseudo mask corresponding to category index  $c$  is formulated as:

$$m_0 = s * \lfloor c/k^2 \rfloor, \quad m_1 = s * \lfloor (c - m_0 * k^2)/k \rfloor, \quad m_2 = s * (c - m_0 * k^2 - m_1 * k), \quad (7)$$

where  $s * (k - 1) < 255$  and  $\lfloor \cdot \rfloor$  means the floor operator. The  $(m_0^i, m_1^i, m_2^i)$  are called anchors.

After the transformation, we adopt a VAE encoder  $\mathcal{E}$  to compress the images and pseudo masks into the latent space. The corresponding VAE decoder  $\mathcal{D}$  restores the latent variables to the pixel space.

$$z_0 = \mathcal{E}(I), \quad z_1 = \mathcal{E}(M), \quad \tilde{I} = \mathcal{D}(\tilde{z}_0), \quad \tilde{M} = \mathcal{D}(\tilde{z}_1), \quad (8)$$

where  $\tilde{z}$  means the output of the UNet.

**Discussion.** Although previous works [71] argue that segmentation masks are lower in entropy and specifically re-train a lighter network, we still adopt the off-the-shelf VAE from SD. The reasons are as follows: 1) The number of parameters in VAE is negligible compared to the UNet (84M vs. 860M). 2) The VAE specifically trained for segmentation masks can not be applied to images, thus destroying the bi-directional transportation. 3) Specific training creates spatial priors, such as clustering, which hinders our exploration of LDM’s segmentation capability itself.

Note that we do not use image captions or image features as prompts. As our model unifies semantic segmentation and image synthesis with *one* model, the usage of captions contradicts the definition of semantic segmentation task while the latter is non-casual for image synthesis. Thus, in this work, we set the prompt as empty.

**Bi-directional Training and Inference.** Contrary to the conventional approach, we propose modeling the segmentation task with rectified flow. It is an ODE framework that aims to learn the mapping between two distributions through straight trajectories.

Denote  $\pi_0$  and  $\pi_1$  represent the distribution of the latent variables of images and masks, respectively. Denote  $z_0 \sim \pi_0$  and  $z_1 \sim \pi_1$ , the trajectory from  $z_0$  to  $z_1$  can be formulated as  $z_t = \varphi_t(z_0, z_1)$ :

$$\frac{dz_t}{dt} = \frac{\partial \varphi_t(z_0, z_1)}{\partial t}. \quad (9)$$

When  $\varphi$  is the trajectory of rectified flow [43],  $z_t$  can be reformulated as the linear interpolation between  $z_0$  and  $z_1$  as  $z_t = (1 - t)z_0 + tz_1$ . We aim to learn the velocity field using neural networks  $v_\theta(z_t, t)$  and solve it with optimization methods,

$$\begin{aligned} \mathcal{L} &= \int_0^1 \mathbb{E}_{(z_0, z_1) \sim \gamma} \left[ \left\| v_\theta(z_t, t) - \frac{\partial \varphi_t(z_0, z_1)}{\partial t} \right\|^2 \right] dt, \\ &= \int_0^1 \mathbb{E}_{(z_0, z_1) \sim \gamma} \left[ \|v_\theta(z_t, t) - (z_1 - z_0)\|^2 \right] dt, \end{aligned} \quad (10)$$

where  $\gamma$  indicates the coupling of images and their corresponding pseudo masks.

Eq. 10 is our training loss. Upon training completed, the transfer from  $z_0$  to  $z_1$  can be described via an ODE:

$$\frac{dz_t}{dt} = v_\theta(z_t, t), \quad t \in [0, 1]. \quad (11)$$

So far, we have constructed a mapping from the distribution of images to that of masks. Compared with DSMs in Eq. 6, our approach avoids the interference of randomness, enabling the application of diffusion models to semantic segmentation tasks.

Moreover, Eq. 10 has a time-symmetric form, which results in an equivalent problem by exchanging  $z_0$  and  $z_1$  and flipping the sign of  $v_\theta$ . Interestingly, the transportation problem from  $\pi_1$  to  $\pi_0$  indicates the semantic image synthesis task. This means that semantic segmentation and semantic image synthesis essentially become a pair of mutually reverse problems that share the same ODE (Eq. 11) and have solutions with opposite signs.

In the inference stage, we can obtain the approximate results by numerical solvers like the forward Euler method, which can be formulated as follows,

Semantic segmentation is regarded as the transportation from  $z_0$  to  $z_1$ , which we call *forward flow*. The ODE is Eq. 11 and the numerical solution is,

$$z_{t+\frac{1}{N}} = z_t + \frac{1}{N}v_\theta(z_t, t), \quad t \in \{0, 1, \dots, N-1\}/N. \quad (12)$$

After  $\tilde{M}$  is restored with Eq. 8, we calculate the L2 distance between  $\tilde{M}$  and anchors and obtain the segmentation mask.

Correspondingly, the semantic image synthesis task is considered to transfer in a reverse direction, which we call the *reverse flow*. Specifically, this transfer can be described as  $\frac{dz_t}{dt} = -v_\theta(z_t, t)$ , and the solution is,

$$z_{t-\frac{1}{N}} = z_t - \frac{1}{N}v_\theta(z_t, t), \quad t \in \{N, N-1, \dots, 1\}/N. \quad (13)$$

### 3.3 Finite Perturbation

In Eq. 10, the model is configured to learn the one-to-one mapping between images and masks. However, assigning a fixed mask to each image brings about several problems. First, we find that constant  $z_1$  in Eq. 13 hinders the multi-modal generation for the image synthesis task. Moreover, the pseudo masks are low in entropy. We hypothesize that the low-entropy distribution of masks hinders the training process and may finally spoil the quality of synthesis results.

To this end, we propose to add finite perturbation on the pseudo masks. Specifically, given pseudo masks  $M$  which has a spacing of  $s$ , we add a noise with a limited amplitude on  $M$ ,

$$M' = M + \epsilon, \quad \epsilon \sim U(-\beta, \beta), \quad (14)$$

where  $U$  is a uniform distribution. We set  $0 < \beta < s/2$  to ensure that the semantic label of each pixel does not change. Therefore, we propose to replace  $z_1$  with  $z'_1 = \mathcal{E}(M')$  in Eq. 10 and Eq. 13. We show the effectiveness of this design in Sec. 4.3.

## 4 Experiments

### 4.1 Experimental Settings

**Dataset and Metrics.** We study SemFlow using three popular datasets: COCO [40], CelebAMask-HQ [29], and Cityscapes [12]. They contain 133, 19, and 19 categories, respectively. The train/val splits follow the setting of these datasets. For semantic segmentation, we evaluate with mean intersection over union (mIoU). For semantic image synthesis, we assess with the Fréchet inception distance (FID) [22] and learned perceptual image patch similarity (LPIPS) [86]. We also evaluate the quality of synthesized images by calculating mIoU with DRN-D-105 [83] model.

**Implementation Details.** The SemFlow model is built upon Stable Diffusion UNet and initialized with weights from the pre-trained SD 1.5. Images and semantic masks in COCO, CelebAMask-HQ,

Table 1: **Semantic segmentation results on COCO dataset.** SS and SIS represents semantic segmentation and semantic image synthesis, respectively. **Sampler-N** means the usage of a specific sampler with N inference steps. Mask2Former ( $\dagger$ ) is trained with a resolution of  $1024 \times 1024$ .

Method	Task		Sampler	mIoU
	SS	SIS		
Mask2Former $\dagger$ [10]	✓		-	61.5
DSM [61]	✓		DDIM-50	23.1
DSM [61]	✓		DDPM-50	27.5
SemFlow (ours)	✓	✓	Euler-10	49.2

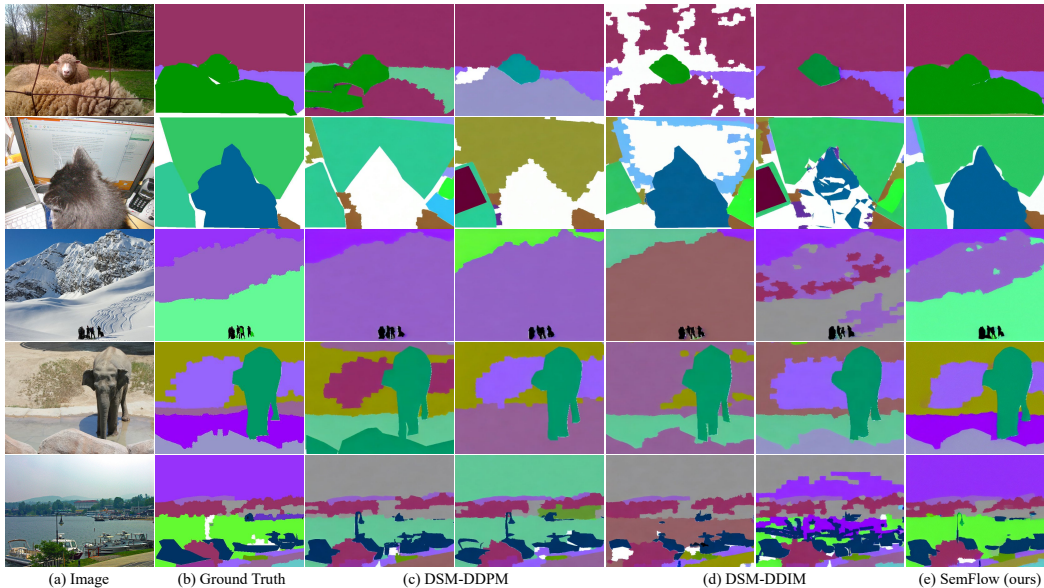


Figure 2: **Semantic segmentation results on COCO dataset.** For the ground truth, each color reflects the value of anchors (Eq. 7), which corresponds to one semantic category, and the color white indicates the ignored regions. The predictions of DSM vary considerably under different random seeds.

and Cityscapes are resized and cropped into  $512 \times 512$ ,  $512 \times 512$ , and  $512 \times 1024$ , and trained for 80K, 80K, and 8K iterations, respectively. The batch size is 256. We use the off-the-shelf VAE of the corresponding Stable Diffusion model. The spacing  $s$  is set as 50, and the division coefficient  $k$  is 6. We use the AdamW optimizer with  $1 \times 10^{-3}$  weight decay. The initial learning rate is  $1 \times 10^{-4}$ ,  $5 \times 10^{-5}$ , and  $2 \times 10^{-5}$  for COCO, Cityscapes, and CelebAMask-HQ, respectively. All experiments are conducted on 8 NVIDIA A100 GPUs. Note that there is no need to train two models for segmentation and synthesis separately since the optimization target in Eq. 10 is time-symmetric.

**Baselines.** We seek to unify semantic segmentation (SS) and semantic image synthesis (SIS) into a pair of reverse problems and train *one* model for a solution. As few previous works achieve this goal, we thus take different baselines for SS and SIS, respectively. For SS, we design two baseline models, DSMs [61], which follow the principle of diffusion-based conditional generation modeling in Sec. 3.1. The network structure and hyperparameters of DSM follow SemFlow, except that the inputs of UNet are 8 channels. Specifically, the noise and images are concatenated in the channel dimension. DSM-DDIM and DSM-DDPM differ in differential equation modeling (ODE vs. SDE). For SIS, we take pix2pixHD [74], SPADE [56], SC-GAN [76], BBDM [30] and CycleGAN [91] as the baselines.

## 4.2 Main Results

**Semantic Segmentation.** Fig. 2 shows the qualitative comparison between SemFlow and DSMs. Our SemFlow demonstrates satisfactory performance in a range of scenarios and exhibits high accuracy

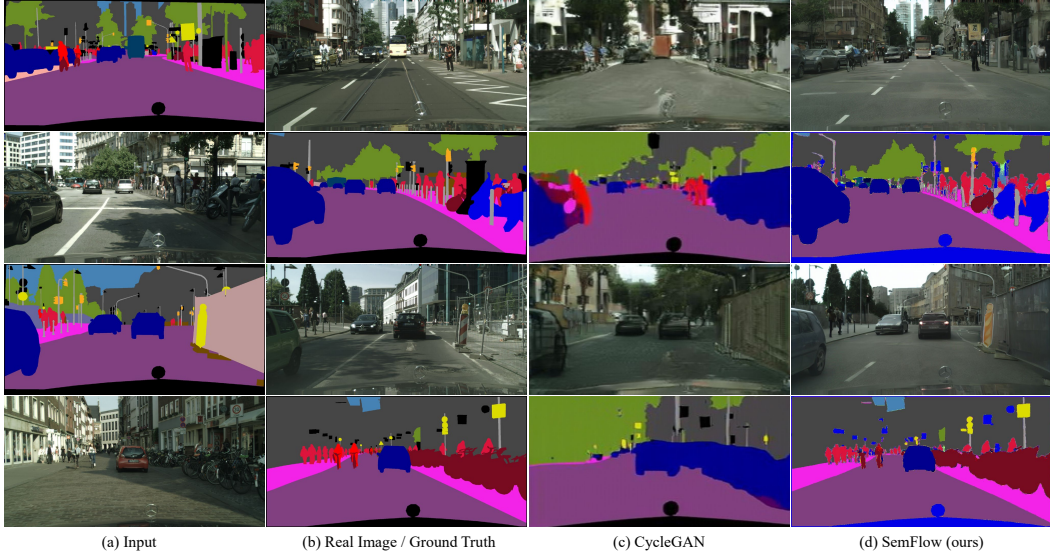


Figure 3: **Semantic segmentation and semantic image synthesis results on Cityscapes dataset.** The color black in the ground truth indicates the ignored region. The segmentation results of SemFlow are colored following [12].

Table 2: **Quantitative results for semantic image synthesis.** SS and SIS represents semantic segmentation and semantic image synthesis, respectively.

Method	Task		CelebAMask-HQ		Cityscapes	
	SS	SIS	FID	LPIPS	mIoU	FID
pix2pixHD [74]		✓	54.7	0.529	58.3	95.0
SPADE [56]		✓	42.2	0.487	62.3	71.8
SC-GAN [76]		✓	19.2	0.395	66.9	49.5
BBDM [30]		✓	21.4	0.370	N/A	N/A
SemFlow (ours)	✓	✓	32.6	0.393	61.8	40.2

in classifying the semantic labels of targets. In contrast, DSM fails in semantic segmentation tasks, regardless of SDE or ODE modeling. First, DSM is inferior to SemFlow in discriminating different semantic categories. Moreover, the outputs of DSM-DDIM and DSM-DDPM change dramatically with different random seeds. As discussed in Sec. 3.1, DSM is susceptible to the randomness inherent in diffusion models, making it unable to produce deterministic results.

Tab. 1 shows the quantitative results on the COCO dataset. We compare SemFlow with two variants of DSM and choose Mask2Former as the upper bound, which is a strong discriminative segmentation model. Regarding accuracy, our SemFlow achieves 49.2 mIoU and outperforms DSMs by a remarkable margin. Moreover, SemFlow only uses a simple sampler, forward Euler method, and fewer inference steps than DSMs. Further reducing the inference steps brings about faster generation but witnesses a slight drop in performance, which is analyzed in Sec. 4.3.

**Semantic Image Synthesis.** We compare our approach with other specialist models on semantic image synthesis tasks in Tab. 2. On CelebAMask-HQ, SemFlow achieves a performance of 32.6 FID and 0.393 LPIPS. On Cityscapes, our approach improves urban streets synthesis to FID of 40.2, compared to FID of SC-GAN 49.5.

Beyond specialist models, we also qualitatively compare our approach with CycleGAN [91] in Fig. 3 to demonstrate the *overall* performance on SS and SIS tasks. All results of SemFlow are generated with *one* model. In other words, the ODE modeling of SS and SIS share the same velocity field and only differ in the sign. The first and third rows show the image synthesis results given semantic layouts, while the second and fourth row shows the segmentation results. Our synthesis and

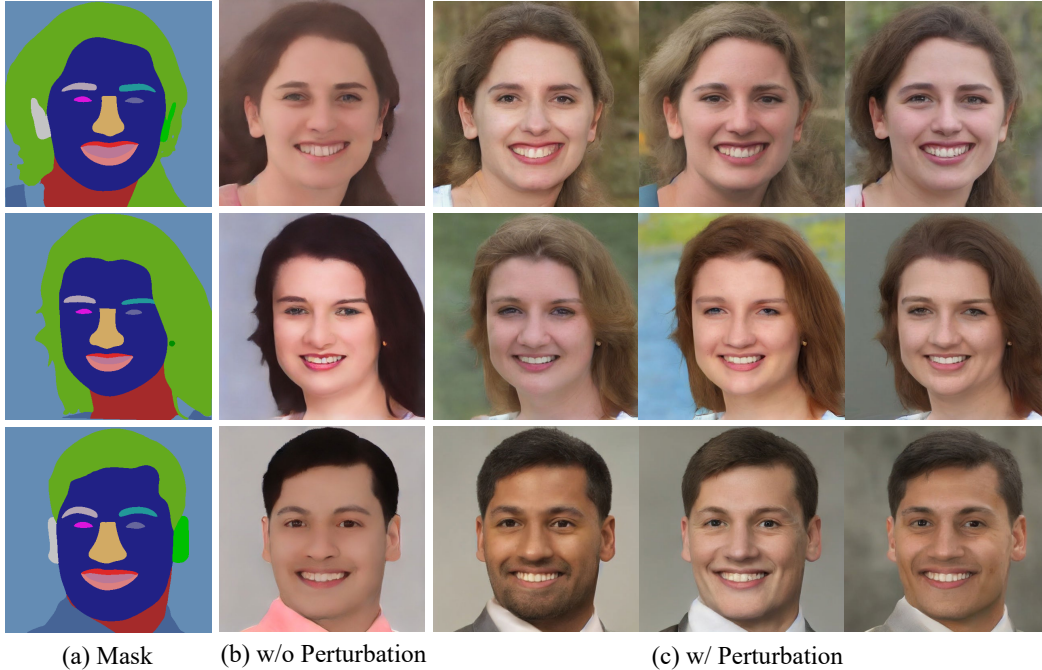


Figure 4: **Semantic image synthesis results on FFHQ dataset.** Semantic masks are colored to show different semantic components. SemFlow w/ Perturbation indicates the finite perturbation operation in Eq. 14.

segmentation results are inspiring and significantly outperform CycleGAN. Note that CycleGAN essentially trains two unidirectional generators while we employ only *one* model for the two tasks.

**Discussion.** Although the performance gap exists compared with Mask2Former, our approach solves the two major issues of diffusion-based segmentation models: 1) Randomness of outputs and 2) large inference steps. We believe it significantly reduces the gap between discriminative models and diffusion models.

### 4.3 Ablation Studies

**Perturbation.** Fig. 4 shows the synthesized results of SemFlow on the FFHQ [27] dataset and demonstrates the importance of perturbation operation. First, perturbation enables our approach to generate multi-modal results from one semantic layout using different noises. The synthesized results show diverse appearances, such as skin, hair color, and the background, and exhibit good consistency with the masks. Moreover, we also show the synthesis results of the model without perturbation in Fig. 4. It is witnessed that the model without perturbation is only able to generate uni-modal results, and the synthesized images exhibit a loss of detail and suffer from severe over-smoothing problems.

**Straight Trajectory.** Our SemFlow aims to establish linear trajectories between the distribution of images and the masks, which enables it to sample with fewer steps.

Tab. 3 compares the performance of DSM and SemFlow on segmentation tasks under different inference steps, where DSM sampled with DDPM and DDIM represent SDE and ODE modeling, respectively. Overall, SemFlow outperforms DSM by a remarkable margin regardless of the inference steps. Specifically, the DSMs’ performance declines markedly as the number of steps decreases. With 5 steps, the DSM-DDPM achieves a mIoU of 10.1, while the DSM-DDIM achieves 7.5 mIoU. On the contrary, our SemFlow achieves 35.9 even with one step.

Fig. 5 provides synthesis results of FFHQ with different inference steps. Although fewer steps will result in some loss of detail and make the images appear smoother, the results of one-step synthesis are still competitive. This indicates that the trajectory between the two distributions is straightened.

Fig.6 and Fig. 7 visualize the latent variable sampled from the trajectory. The transition between  $z_0$  and  $z_1$  is smooth.

Table 3: **Semantic segmentation results with different inference steps on COCO dataset.** mIoU is used as the metric.

Method&Sampler		1	2	5	10	25	50	100	200
DSM	DDIM	-	0.2	7.5	15.6	20.4	23.1	24.2	22.9
	DDPM	-	0.2	10.1	19.5	26.1	27.5	28.8	29.3
SemFlow	Euler	35.9	41.5	48.0	49.2	48.7	48.2	47.9	46.8

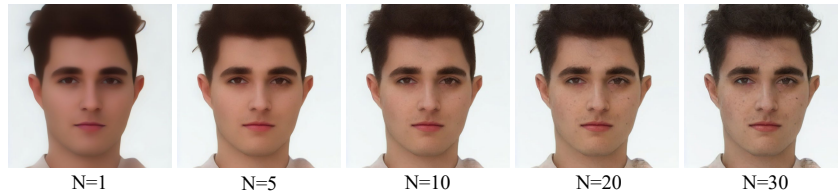


Figure 5: **Synthesis results with different inference steps on FFHQ dataset.** We use the forward Euler method to get numerical solutions. Our approach obtains competitive results even with only one inference step.



Figure 6: **Visualization of latent variables on the trajectory from  $z_1$  to  $z_0$  (Semantic image synthesis).** Top row: COCO. Bottom row: Cityscapes.



Figure 7: **Visualization of latent variables on the trajectory from  $z_0$  to  $z_1$  (Semantic segmentation).** Top row: COCO. Bottom row: Cityscapes.

## 5 Conclusion

In this work, we present SemFlow, a framework that employs a diffusion model to integrate semantic segmentation and semantic image synthesis as a pair of reverse problems. To overcome the contradiction between the randomness of diffusion models and the certainty of semantic segmentation results, we propose to model semantic segmentation as a transport problem between image and mask distributions. We then employ rectified flow to learn the transfer function, which brings the benefits of

reversible transportation. We propose a finite perturbation method to enable multi-modal generation, which also greatly improves the quality of synthesized results. With straight trajectory modeling, our model can sample with much fewer steps. Experimental results show that even with a weak sampler, our model still achieves comparable or even better results than specialist models. We hope our research can inspire the findings on unified generative model design for the community.

**Acknowledgement.** This work is supported by the National Key Research and Development Program of China (No. 2023YFC3807600).

## References

- [1] Michael S Albergo, Nicholas M Boffi, and Eric Vanden-Eijnden. Stochastic interpolants: A unifying framework for flows and diffusions. *arXiv preprint arXiv:2303.08797*, 2023. 2
- [2] Tomer Amit, Tal Shaharbany, Eliya Nachmani, and Lior Wolf. Segdiff: Image segmentation with diffusion probabilistic models. *arXiv preprint arXiv:2112.00390*, 2021. 3
- [3] Dmitry Baranchuk, Ivan Rubachev, Andrey Voynov, Valentin Khruikov, and Artem Babenko. Label-efficient semantic segmentation with diffusion models. In *ICLR*, 2022. 3
- [4] Tim Brooks, Aleksander Holynski, and Alexei A Efros. Instructpix2pix: Learning to follow image editing instructions. In *CVPR*, 2023. 2
- [5] Holger Caesar, Varun Bankiti, Alex H Lang, Sourabh Vora, Venice Erin Liang, Qiang Xu, Anush Krishnan, Yu Pan, Giancarlo Baldan, and Oscar Beijbom. nuscenes: A multimodal dataset for autonomous driving. In *CVPR*, 2020. 1
- [6] JungWoo Chae, Hyunin Cho, Sooyeon Go, Kyungmook Choi, and Youngjung Uh. Semantic image synthesis with unconditional generator. In *NeurIPS*, 2023. 3
- [7] Liang-Chieh Chen, George Papandreou, Iasonas Kokkinos, Kevin Murphy, and Alan L Yuille. Deeplab: Semantic image segmentation with deep convolutional nets, atrous convolution, and fully connected crfs. *TPAMI*, 2017. 1, 3
- [8] Qifeng Chen and Vladlen Koltun. Photographic image synthesis with cascaded refinement networks. In *ICCV*, 2017. 1, 3
- [9] Ting Chen, Lala Li, Saurabh Saxena, Geoffrey Hinton, and David J Fleet. A generalist framework for panoptic segmentation of images and videos. In *ICCV*, 2023. 3
- [10] Bowen Cheng, Ishan Misra, Alexander G Schwing, Alexander Kirillov, and Rohit Girdhar. Masked-attention mask transformer for universal image segmentation. In *CVPR*, 2022. 1, 3, 6
- [11] Bowen Cheng, Alex Schwing, and Alexander Kirillov. Per-pixel classification is not all you need for semantic segmentation. In *NeurIPS*, 2021. 1, 3
- [12] Marius Cordts, Mohamed Omran, Sebastian Ramos, Timo Rehfeld, Markus Enzweiler, Rodrigo Benenson, Uwe Franke, Stefan Roth, and Bernt Schiele. The cityscapes dataset for semantic urban scene understanding. In *CVPR*, 2016. 5, 7
- [13] Prafulla Dhariwal and Alexander Nichol. Diffusion models beat gans on image synthesis. In *NeurIPS*, 2021. 2
- [14] Alexey Dosovitskiy, Lucas Beyer, Alexander Kolesnikov, Dirk Weissenborn, Xiaohua Zhai, Thomas Unterthiner, Mostafa Dehghani, Matthias Minderer, Georg Heigold, Sylvain Gelly, et al. An image is worth 16x16 words: Transformers for image recognition at scale. In *ICLR*, 2021. 3
- [15] Patrick Esser, Sumith Kulal, Andreas Blattmann, Rahim Entezari, Jonas Müller, Harry Saini, Yam Levi, Dominik Lorenz, Axel Sauer, Frederic Boesel, et al. Scaling rectified flow transformers for high-resolution image synthesis. *arXiv preprint arXiv:2403.03206*, 2024. 2
- [16] Zigang Geng, Binxin Yang, Tiankai Hang, Chen Li, Shuyang Gu, Ting Zhang, Jianmin Bao, Zheng Zhang, Han Hu, Dong Chen, et al. Instructdiffusion: A generalist modeling interface for vision tasks. In *CVPR*, 2024. 3
- [17] Ian Goodfellow, Jean Pouget-Abadie, Mehdi Mirza, Bing Xu, David Warde-Farley, Sherjil Ozair, Aaron Courville, and Yoshua Bengio. Generative adversarial networks. *Communications of the ACM*, 2020. 1
- [18] Zhangxuan Gu, Haoxing Chen, Zhuoer Xu, Jun Lan, Changhua Meng, and Weiqiang Wang. Diffusioninst: Diffusion model for instance segmentation. In *ICASSP*, 2024. 3
- [19] Kaiming He, Xiangyu Zhang, Shaoqing Ren, and Jian Sun. Deep residual learning for image recognition. In *CVPR*, 2016. 3
- [20] Eric Heitz, Laurent Belcour, and Thomas Chambon. Iterative  $\alpha$ -(de) blending: A minimalist deterministic diffusion model. In *SIGGRAPH*, 2023. 2
- [21] Amir Hertz, Ron Mokady, Jay Tenenbaum, Kfir Aberman, Yael Pritch, and Daniel Cohen-Or. Prompt-to-prompt image editing with cross attention control. In *ICLR*, 2023. 2
- [22] Martin Heusel, Hubert Ramsauer, Thomas Unterthiner, Bernhard Nessler, and Sepp Hochreiter. Gans trained by a two time-scale update rule converge to a local nash equilibrium. *NeurIPS*, 2017. 5

- [23] Jonathan Ho, Ajay Jain, and Pieter Abbeel. Denoising diffusion probabilistic models. In *NeurIPS*, 2020. 1, 2
- [24] Jonathan Ho, Chitwan Saharia, William Chan, David J Fleet, Mohammad Norouzi, and Tim Salimans. Cascaded diffusion models for high fidelity image generation. *JMLR*, 2022. 2
- [25] Jonathan Ho and Tim Salimans. Classifier-free diffusion guidance. In *NeurIPS Workshops*, 2021. 2
- [26] Phillip Isola, Jun-Yan Zhu, Tinghui Zhou, and Alexei A Efros. Image-to-image translation with conditional adversarial networks. In *CVPR*, 2017. 1, 3
- [27] Tero Karras, Samuli Laine, and Timo Aila. A style-based generator architecture for generative adversarial networks. In *CVPR*, 2019. 8
- [28] Minh-Quan Le, Tam V Nguyen, Trung-Nghia Le, Thanh-Toan Do, Minh N Do, and Minh-Triet Tran. Maskdiff: Modeling mask distribution with diffusion probabilistic model for few-shot instance segmentation. In *AAAI*, 2024. 3
- [29] Cheng-Han Lee, Ziwei Liu, Lingyun Wu, and Ping Luo. Maskgan: Towards diverse and interactive facial image manipulation. In *CVPR*, 2020. 5
- [30] Bo Li, Kaitao Xue, Bin Liu, and Yu-Kun Lai. Bbdm: Image-to-image translation with brownian bridge diffusion models. In *CVPR*, 2023. 6, 7
- [31] Ke Li, Tianhao Zhang, and Jitendra Malik. Diverse image synthesis from semantic layouts via conditional imle. In *ICCV*, 2019. 1, 3
- [32] Xiangtai Li, Henghui Ding, Wenwei Zhang, Haobo Yuan, Guangliang Cheng, Pang Jiangmiao, Kai Chen, Ziwei Liu, and Chen Change Loy. Transformer-based visual segmentation: A survey. *arXiv pre-print*, 2023. 3
- [33] Xinghui Li, Jingyi Lu, Kai Han, and Victor Prisacariu. Sd4match: Learning to prompt stable diffusion model for semantic matching. *arXiv preprint arXiv:2310.17569*, 2023. 3
- [34] Xiangtai Li, Ansheng You, Zhen Zhu, Houlong Zhao, Maoke Yang, Kuiyuan Yang, and Yunhai Tong. Semantic flow for fast and accurate scene parsing. In *ECCV*, 2020. 3
- [35] Xiangtai Li, Haobo Yuan, Wei Li, Henghui Ding, Size Wu, Wenwei Zhang, Yining Li, Kai Chen, and Chen Change Loy. Omg-seg: Is one model good enough for all segmentation? In *CVPR*, 2024. 3
- [36] Xiangtai Li, Jiangning Zhang, Yibo Yang, Guangliang Cheng, Kuiyuan Yang, Yu Tong, and Dacheng Tao. Sfnet: Faster and accurate domain agnostic semantic segmentation via semantic flow. *IJCV*, 2023. 3
- [37] Xiangtai Li, Wenwei Zhang, Jiangmiao Pang, Kai Chen, Guangliang Cheng, Yunhai Tong, and Chen Change Loy. Video k-net: A simple, strong, and unified baseline for video segmentation. In *CVPR*, 2022. 3
- [38] Yuheng Li, Yijun Li, Jingwan Lu, Eli Shechtman, Yong Jae Lee, and Krishna Kumar Singh. Collaging class-specific gans for semantic image synthesis. In *ICCV*, 2021. 3
- [39] Yuheng Li, Haotian Liu, Qingyang Wu, Fangzhou Mu, Jianwei Yang, Jianfeng Gao, Chunyuan Li, and Yong Jae Lee. Gligen: Open-set grounded text-to-image generation. In *CVPR*, 2023. 1, 3
- [40] Tsung-Yi Lin, Michael Maire, Serge Belongie, James Hays, Pietro Perona, Deva Ramanan, Piotr Dollár, and C Lawrence Zitnick. Microsoft coco: Common objects in context. In *ECCV*, 2014. 5
- [41] Yaron Lipman, Ricky TQ Chen, Heli Ben-Hamu, Maximilian Nickel, and Matt Le. Flow matching for generative modeling. In *ICLR*, 2023. 2
- [42] Qiang Liu. Rectified flow: A marginal preserving approach to optimal transport. *arXiv preprint arXiv:2209.14577*, 2022. 2
- [43] Xingchao Liu, Chengyue Gong, and Qiang Liu. Flow straight and fast: Learning to generate and transfer data with rectified flow. In *ICLR*, 2023. 2, 3, 4
- [44] Xihui Liu, Guojun Yin, Jing Shao, Xiaogang Wang, et al. Learning to predict layout-to-image conditional convolutions for semantic image synthesis. In *NeurIPS*, 2019. 3
- [45] Xingchao Liu, Xiwen Zhang, Jianzhu Ma, Jian Peng, et al. InstafLOW: One step is enough for high-quality diffusion-based text-to-image generation. In *ICLR*, 2024. 2, 3
- [46] Ze Liu, Yutong Lin, Yue Cao, Han Hu, Yixuan Wei, Zheng Zhang, Stephen Lin, and Baining Guo. Swin transformer: Hierarchical vision transformer using shifted windows. In *ICCV*, 2021. 3
- [47] Zhuang Liu, Hanzi Mao, Chao-Yuan Wu, Christoph Feichtenhofer, Trevor Darrell, and Saining Xie. A convnet for the 2020s. In *CVPR*, 2022. 3
- [48] Jonathan Long, Evan Shelhamer, and Trevor Darrell. Fully convolutional networks for semantic segmentation. In *CVPR*, 2015. 1
- [49] Andreas Lugmayr, Martin Danelljan, Andres Romero, Fisher Yu, Radu Timofte, and Luc Van Gool. Repaint: Inpainting using denoising diffusion probabilistic models. In *CVPR*, 2022. 2
- [50] Shitong Luo and Wei Hu. Diffusion probabilistic models for 3d point cloud generation. In *CVPR*, 2021. 2
- [51] Shitong Luo and Wei Hu. Score-based point cloud denoising. In *ICCV*, 2021. 2
- [52] Zhengyao Lv, Xiaoming Li, Zhenxing Niu, Bing Cao, and Wangmeng Zuo. Semantic-shape adaptive feature modulation for semantic image synthesis. In *CVPR*, 2022. 3
- [53] Zhaoyang Lyu, Zhifeng Kong, Xudong Xu, Liang Pan, and Dahua Lin. A conditional point diffusion-refinement paradigm for 3d point cloud completion. In *ICLR*, 2022. 2

- [54] Chenlin Meng, Yutong He, Yang Song, Jiaming Song, Jiajun Wu, Jun-Yan Zhu, and Stefano Ermon. Sdedit: Guided image synthesis and editing with stochastic differential equations. In *ICLR*, 2022. 2
- [55] Mehdi Mirza and Simon Osindero. Conditional generative adversarial nets. *arXiv preprint arXiv:1411.1784*, 2014. 1
- [56] Taesung Park, Ming-Yu Liu, Ting-Chun Wang, and Jun-Yan Zhu. Semantic image synthesis with spatially-adaptive normalization. In *CVPR*, 2019. 3, 6, 7
- [57] William Peebles and Saining Xie. Scalable diffusion models with transformers. In *ICCV*, 2023. 2
- [58] Dustin Podell, Zion English, Kyle Lacey, Andreas Blattmann, Tim Dockhorn, Jonas Müller, Joe Penna, and Robin Rombach. Sdxl: Improving latent diffusion models for high-resolution image synthesis. In *ICLR*, 2024. 2
- [59] Lu Qi, Lehan Yang, Weidong Guo, Yu Xu, Bo Du, Varun Jampani, and Ming-Hsuan Yang. Unigs: Unified representation for image generation and segmentation. In *CVPR*, 2024. 1, 2, 3
- [60] Alec Radford, Luke Metz, and Soumith Chintala. Unsupervised representation learning with deep convolutional generative adversarial networks. In *ICLR*, 2016. 1
- [61] Robin Rombach, Andreas Blattmann, Dominik Lorenz, Patrick Esser, and Björn Ommer. High-resolution image synthesis with latent diffusion models. In *CVPR*, 2022. 2, 4, 6
- [62] Olaf Ronneberger, Philipp Fischer, and Thomas Brox. U-net: Convolutional networks for biomedical image segmentation. In *MICCAI*, 2015. 1, 3
- [63] Chitwan Saharia, William Chan, Huiwen Chang, Chris Lee, Jonathan Ho, Tim Salimans, David Fleet, and Mohammad Norouzi. Palette: Image-to-image diffusion models. In *SIGGRAPH*, 2022. 2
- [64] Chitwan Saharia, Jonathan Ho, William Chan, Tim Salimans, David J Fleet, and Mohammad Norouzi. Image super-resolution via iterative refinement. *TPAMI*, 2022. 2
- [65] Tim Salimans, Ian Goodfellow, Wojciech Zaremba, Vicki Cheung, Alec Radford, and Xi Chen. Improved techniques for training gans. In *NeurIPS*, 2016. 1
- [66] Jiaming Song, Chenlin Meng, and Stefano Ermon. Denoising diffusion implicit models. In *ICLR*, 2021. 1, 2, 3
- [67] Yang Song, Jascha Sohl-Dickstein, Diederik P Kingma, Abhishek Kumar, Stefano Ermon, and Ben Poole. Score-based generative modeling through stochastic differential equations. In *ICLR*, 2021. 1, 2
- [68] Vadim Sushko, Edgar Schönfeld, Dan Zhang, Juergen Gall, Bernt Schiele, and Anna Khoreva. You only need adversarial supervision for semantic image synthesis. In *ICLR*, 2021. 3
- [69] Zhentao Tan, Menglei Chai, Dongdong Chen, Jing Liao, Qi Chu, Bin Liu, Gang Hua, and Nenghai Yu. Diverse semantic image synthesis via probability distribution modeling. In *CVPR*, 2021. 3
- [70] Hao Tang, Song Bai, and Nicu Sebe. Dual attention gans for semantic image synthesis. In *ACM MM*, 2020. 3
- [71] Wouter Van Gansbeke and Bert De Brabandere. A simple latent diffusion approach for panoptic segmentation and mask inpainting. *arXiv preprint arXiv:2401.10227*, 2024. 2, 3, 4
- [72] Qiang Wan, Zilong Huang, Bingyi Kang, Jiashi Feng, and Li Zhang. Harnessing diffusion models for visual perception with meta prompts. *arXiv preprint arXiv:2312.14733*, 2023. 3
- [73] Chaoyang Wang, Xiangtai Li, Henghui Ding, Lu Qi, Jiangning Zhang, Yunhai Tong, Chen Change Loy, and Shuicheng Yan. Explore in-context segmentation via latent diffusion models. *arXiv preprint arXiv:2403.09616*, 2024. 3
- [74] Ting-Chun Wang, Ming-Yu Liu, Jun-Yan Zhu, Andrew Tao, Jan Kautz, and Bryan Catanzaro. High-resolution image synthesis and semantic manipulation with conditional gans. In *CVPR*, 2018. 1, 3, 6, 7
- [75] Weilun Wang, Jianmin Bao, Wengang Zhou, Dongdong Chen, Dong Chen, Lu Yuan, and Houqiang Li. Semantic image synthesis via diffusion models. *arXiv preprint arXiv:2207.00050*, 2022. 3
- [76] Yi Wang, Lu Qi, Ying-Cong Chen, Xiangyu Zhang, and Jiaya Jia. Image synthesis via semantic composition. In *ICCV*, 2021. 3, 6, 7
- [77] Jiahao Xie, Wei Li, Xiangtai Li, Ziwei Liu, Yew Soon Ong, and Chen Change Loy. Mosaicfusion: Diffusion models as data augmenters for large vocabulary instance segmentation. *arXiv preprint arXiv:2309.13042*, 2023. 3
- [78] Guangkai Xu, Yongtao Ge, Mingyu Liu, Chengxiang Fan, Kangyang Xie, Zhiyue Zhao, Hao Chen, and Chunhua Shen. Diffusion models trained with large data are transferable visual models. *arXiv preprint arXiv:2403.06090*, 2024. 3
- [79] Jiarui Xu, Sifei Liu, Arash Vahdat, Wonmin Byeon, Xiaolong Wang, and Shalini De Mello. Open-vocabulary panoptic segmentation with text-to-image diffusion models. In *CVPR*, 2023. 3
- [80] Han Xue, Zhiwu Huang, Qianru Sun, Li Song, and Wenjun Zhang. Freestyle layout-to-image synthesis. In *CVPR*, 2023. 3
- [81] Dingdong Yang, Seunghoon Hong, Yunseok Jang, Tianchen Zhao, and Honglak Lee. Diversity-sensitive conditional generative adversarial networks. In *ICLR*, 2019. 3
- [82] Ruihan Yang, Prakhar Srivastava, and Stephan Mandt. Diffusion probabilistic modeling for video generation. *Entropy*, 2023. 2

- [83] Fisher Yu, Vladlen Koltun, and Thomas Funkhouser. Dilated residual networks. In *CVPR*, 2017. 5
- [84] Xiaohui Zeng, Arash Vahdat, Francis Williams, Zan Gojcic, Or Litany, Sanja Fidler, and Karsten Kreis. Lion: Latent point diffusion models for 3d shape generation. In *NeurIPS*, 2022. 2
- [85] Lvmin Zhang, Anyi Rao, and Maneesh Agrawala. Adding conditional control to text-to-image diffusion models. In *ICCV*, 2023. 2
- [86] Richard Zhang, Phillip Isola, Alexei A Efros, Eli Shechtman, and Oliver Wang. The unreasonable effectiveness of deep features as a perceptual metric. In *CVPR*, 2018. 5
- [87] Hengshuang Zhao, Jianping Shi, Xiaojuan Qi, Xiaogang Wang, and Jiaya Jia. Pyramid scene parsing network. In *CVPR*, 2017. 1, 3
- [88] Wenliang Zhao, Yongming Rao, Zuyan Liu, Benlin Liu, Jie Zhou, and Jiwen Lu. Unleashing text-to-image diffusion models for visual perception. In *ICCV*, 2023. 3
- [89] Linqi Zhou, Yilun Du, and Jiajun Wu. 3d shape generation and completion through point-voxel diffusion. In *ICCV*, 2021. 2
- [90] Zongwei Zhou, Md Mahfuzur Rahman Siddiquee, Nima Tajbakhsh, and Jianming Liang. Unet++: A nested u-net architecture for medical image segmentation. In *MICCAI*, 2018. 1
- [91] Jun-Yan Zhu, Taesung Park, Phillip Isola, and Alexei A Efros. Unpaired image-to-image translation using cycle-consistent adversarial networks. In *ICCV*, 2017. 1, 3, 6, 7
- [92] Peihao Zhu, Rameen Abdal, Yipeng Qin, and Peter Wonka. Sean: Image synthesis with semantic region-adaptive normalization. In *CVPR*, 2020. 3
- [93] Zhen Zhu, Zhiliang Xu, Ansheng You, and Xiang Bai. Semantically multi-modal image synthesis. In *CVPR*, 2020. 3